Use of a Site-Directed Triple Mutant To Trap Intermediates: Demonstration That the Flavin C(4a)–Thiol Adduct and Reduced Flavin Are Kinetically Competent Intermediates in Mercuric Ion Reductase†

Susan M. Miller,*,‡ Vincent Massey,‡ David Ballou,‡ Charles H. Williams, Jr.,‡,§ Mark D. Distefano,∥,⊥ Melissa J. Moore,∥,# and Christopher T. Walsh∥

Department of Biological Chemistry, University of Michigan, Ann Arbor, Michigan 48109-0606, VA Medical Center, Ann Arbor, Michigan 48105, and Department of Biological Chemistry and Molecular Pharmacology, Harvard Medical School, Boston, Massachusetts 02115

Received September 1, 1989; Revised Manuscript Received November 6, 1989

ABSTRACT: A mutant form of mercuric reductase, which has three of its four catalytically essential cysteine residues replaced by alanines (ACAA: $Ala_{135}Cys_{140}Ala_{558}Ala_{559}$), has been constructed and used for mechanistic investigations. With disruption of the Hg(II) binding site, the mutant enzyme is devoid of Hg(II) reductase activity. However, it appears to fold properly since it binds FAD normally and exhibits very tight binding of pyridine nucleotides as is seen with the wild-type enzyme. This mutant enzyme allows quantitative accumulation of two species thought to function as intermediates in the catalytic sequence of the flavoprotein disulfide reductase family of enzymes. NADPH reduces the flavin in this mutant, and a stabilized E–$FADH^-$ form accumulates. The second intermediate is a flavin C(4a)–Cys_{140} thiol adduct, which is quantitatively accumulated by reaction of oxidized ACAA enzyme with $NADP^+$. The conversion of the Cys_{135}–Cys_{140} disulfide in wild-type enzyme to the monothiol Cys_{140} in ACAA and the elevated pK_a of Cys_{140} (6.7 vs 5.0 in wild type) have permitted detection of these intermediates at low pH (5.0). The rates of formation of E–$FADH^-$ and the breakdown of the flavin C(4a)–thiol adduct have been measured and indicate that both intermediates are kinetically competent for both the reductive half-reaction and turnover by wild-type enzyme. These results validate the general proposal that electrons flow from NADPH to $FADH^-$ to C(4a)–thiol adduct to the FAD/dithiol form that accumulates as the EH_2 form in the reductive half-reaction for this class of enzymes.

The flavoprotein disulfide reductase enzymes, which include lipoamide dehydrogenase, glutathione reductase, thioredoxin reductase, mercuric reductase, and trypanothione reductase, have several common structural and mechanistic characteristics. With the exception of thioredoxin reductase, they all react with NAD(P)H to form two electron reduced species (EH_2),[1] which can be characterized by their long-wavelength spectral properties (Williams, 1976). This feature has been attributed to a charge-transfer interaction between a thiolate and the oxidized flavin (Searls et al., 1961; Massey & Ghisla, 1974; Matthews & Williams, 1976). It has long been assumed that EH_2 is formed in several steps depicted by Scheme IA. First, NAD(P)H is bound to form a Michaelis complex [E–NAD(P)H]. Then, the flavin is reduced to form E–$FADH^-$. Electron transfer to the disulfide is thought to occur via a C(4a)–thiol adduct of the flavin (Scheme II), leading to the EH_2–$NAD(P)^+$ species that exhibits the charge–transfer spectrum (Thorpe & Williams, 1981). This hypothesis (Hemmerich, 1968; Hamilton, 1971) is supported by model studies (Loechler & Hollocher, 1975; Yokoe & Bruice, 1975; Hevesi & Bruice, 1973; Walker et al., 1970).

Most of these enzymes carry out this complete process extremely rapidly. Lipoamide dehydrogenase is reduced to EH_2 by NADH at rates of $>1000\ s^{-1}$, and no intermediates are observable (Massey et al., 1960; Matthews & Williams, 1976). Reduction of glutathione reductase and mercuric reductase by NADPH at 5 °C is also fast, but the only spectrally identifiable intermediates are very rapidly formed complexes between oxidized flavin and NADPH and between EH_2 and pyridine nucleotide (Bulger & Brandt, 1971; Huber & Brandt, 1980; Sahlman et al., 1984).

Although it is chemically sensible for the process to proceed via a reduced flavin intermediate, kinetic studies have not provided conclusive evidence for its transient existence. In the case of glutathione reductase (Huber & Brandt, 1980), some transient reduction occurs, but the spectrum was not characterized well enough to distinguish whether the intermediate was actually reduced flavin or perhaps a C(4a)-adduct. The flavin C(4a)-adduct has been observed under three conditions: (a) Monoalkylated lipoamide dehydrogenase binds NAD^+ and stabilizes about 50% of a species proposed to be the C(4a) adduct (Thorpe & Williams, 1976, 1981). (b) Two electron reduced thioredoxin reductase substituted with 1-deaza-FAD stabilizes ≈40% of a flavin C(4a)-derivative at low pH

† This work was supported by NIH Grants GM-11106 (V.M.), GM-20877 (D.B.), GM-21444 (C.H.W.), and GM-21643 (C.T.W). M.J.M. was a recipient of an NSF graduate fellowship.

* Author to whom correspondence should be addressed.
‡ University of Michigan.
§ VA Medical Center.
∥ Harvard Medical School.
⊥ Present address: Department of Chemistry, California Institute of Technology, Pasadena, CA 91125.
Present address: Center for Cancer Research, Massachusetts Institute of Technology, Cambridge, MA 02139.

[1] Abbreviations: ACAA, mercuric reductase mutant in which three of the four catalytically essential cysteines (Cys_{135}, Cys_{140}, Cys_{558}, and Cys_{559}, denoted in order by C) have been replaced with alanines as denoted by A; AACC, mercuric reductase mutant with alanines at residues 135 and 140; bp, base pair(s); C-T, charge transfer; EH_2, two electron reduced enzyme; IPTG, isopropyl β-D-thiogalactopyranoside; *merA*, gene encoding mercuric reductase; PAGE, polyacrylamide gel electrophoresis; SDS, sodium dodecyl sulfate.

0006-2960/90/0429-2831$02.50/0

Scheme I: (A) Reduction of the Active Site Disulfide of Disulfide Oxidoreductases and (B) Reactions of ACAA at pH 5 with Pyridine Nucleotides

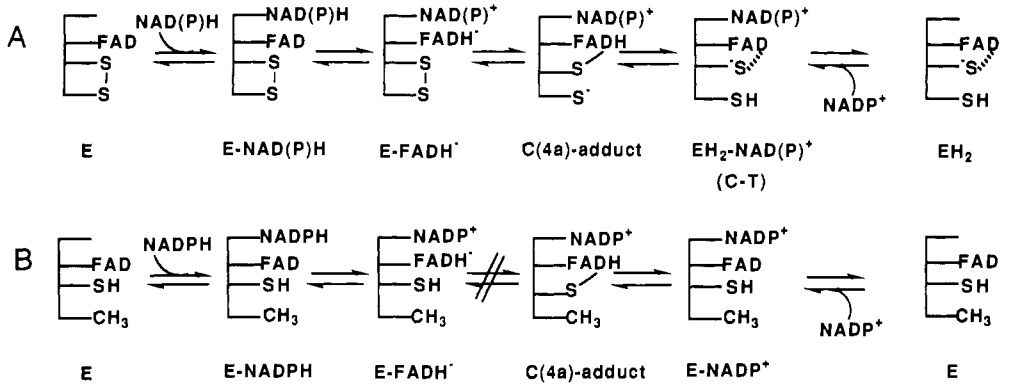

Scheme II: Formation of the Flavin C(4a)–Thiol Adduct

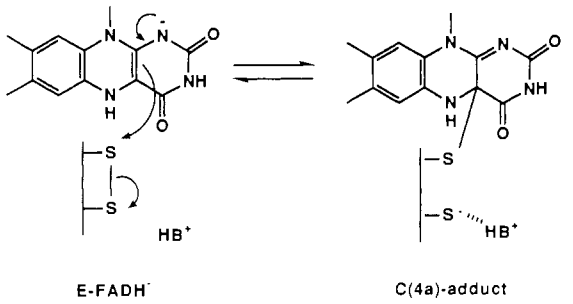

(O'Donnell & Williams, 1984). (c) At low pH (5.1) mercuric reductase reacts rapidly with NADPH to transiently form an estimated 70% of a species with spectral properties like those of a flavin C(4a)-adduct (Sahlman et al., 1986). In all cases, the spectrum of the adduct could only be estimated by extrapolation.

It has now become possible to test the mechanism of Scheme IA more directly in mercuric reductase, a bacterial flavoprotein involved in detoxification of Hg^{2+} in the environment. In addition to the redox-active disulfide, functional in all members of this enzyme family (as depicted in Scheme IA), mercuric reductase has two thiols near the C-terminus, Cys_{558} and Cys_{559} (Brown et al., 1983), that must be present as thiols for the enzyme to be active; at least one of them participates in catalysis (Miller et al., 1989).

Several site-directed mutants of mercuric reductase have been produced and characterized (Schultz et al., 1985; Moore & Walsh, 1989; Distefano et al., 1989). These proteins have mutations at the active site cysteine residues with replacement by alanine or serine. In general, they are all essentially inactive toward reduction of Hg(II); however, like the wild-type enzyme, they react extremely rapidly with NADPH to form charge-transfer complexes, and they also exhibit the normal transhydrogenation and oxidase activities.

One of the mutants, in which Cys_{135}, Cys_{558}, and Cys_{559}, three of the catalytically essential cysteines, have been mutated to alanine residues, is referred to as ACAA. It is particularly useful in delineating various features of the mechanism of the reduction by NADPH, since the protein has only one thiol at the active site, Cys_{140}, which is the thiol participating in the charge-transfer interaction with the FAD (Schultz et al., 1985).[2] It is thus similar to the case of lipoamide dehydrogenase in which the thiol analogous to Cys_{135} in mercuric reductase was alkylated and which was shown to form ca. 50% of a flavin C(4a)–thiol adduct in the presence of NAD^+ (Thorpe & Williams, 1976). The reductive half-reaction for ACAA analogous to that for wild-type flavoprotein disulfide oxidoreductases (Scheme IA) is depicted in Scheme IB. We considered the possibility that mercuric reductase ACAA would have properties similar to those of wild-type enzyme and might be a good system for studying the formation of a flavin C(4a)–thiol adduct upon reaction of the enzyme with $NADP^+$ in the reverse direction. According to the mechanism of Scheme IA, further reaction of the C(4a)-adduct in the ACAA mutant to form reduced flavin ($E–FADH^-$) should be blocked (Scheme IB). Additionally, since at low pH the protonated thiol could not be a charge-transfer donor to the flavin, we felt that the reaction with NADPH in the forward direction would more readily lead to an accumulation of reduced flavin ($E–FADH^-$), a postulated intermediate in the overall reduction path, which could not be observed with wild-type forms of these enzymes. Again, further reaction of $E–FADH^-$ with the remaining active site thiol to form the C(4a)-adduct will not occur with this mutant. We report here kinetic and spectral studies of this enzyme showing that the accumulation of these intermediates is indeed complete and rapid, results that strongly support the hypotheses in Scheme I.

Experimental Procedures

Materials

Restriction enzymes were obtained from New England Biolabs, Bethesda Research Laboratories, or Boehringer Mannheim. T4 DNA ligase and *Escherichia coli* JM105 were obtained from New England Biolabs. AMV reverse transcriptase and calf intestinal phosphatase were purchased from Boehringer Mannheim. Plasmids pMMa558a559 (Moore & Walsh, 1989), pKAM1 (Distefano et al., 1989), and pSE181 and *E. coli* strain W3110 *lacI*^{q} (Schultz et al., 1985) were described previously. All chemicals were of the highest grade available and were used without further purification.

Methods

Routine DNA manipulations were performed as described by Maniatis et al. (1982). UV–visible absorbance spectra were recorded with a Cary 219 double-beam spectrophotometer or a Hewlett-Packard 8452A diode array spectrophotometer. Fluorescence spectra were recorded with a scanning ratio spectrofluorometer built by Gordon Ford and Dr. David Ballou at the University of Michigan. Rapid-reaction studies were carried out by measuring the absorbance with a stopped-flow spectrophotometer with scanning capabilities (2-cm optical

[2] The single mutant ACCC has also been made (Distefano et al., 1989) but in preliminary analysis showed sufficient negative cooperativity behavior for the two subunits in the homodimeric enzyme that it was much less suitable than ACAA for the studies reported here.

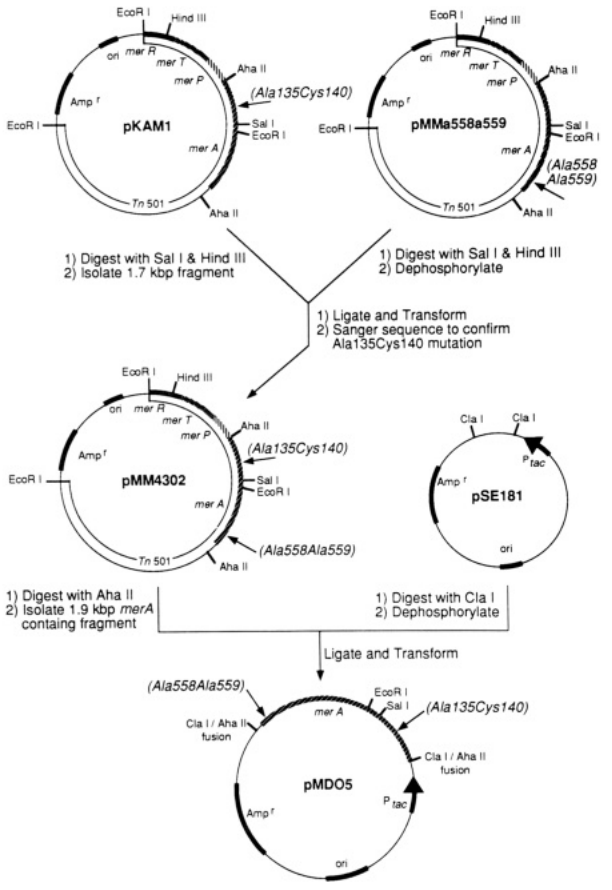

FIGURE 1: Strategy employed for the construction of the plasmid that expresses the ACAA triple mutant mercuric reductase. The construction of pMDO5, which expresses the ACAA mutant mercuric reductase, is shown. The positions of the Ala_{135}, Ala_{558}, and Ala_{559} mutations within the *merA* gene are designated by arrows.

path) as previously described (Beaty & Ballou, 1981) or by measuring the fluorescence with a stopped-flow apparatus from Kinetic Instruments, Inc. (Ann Arbor, MI) and a detection system built by Dr. David Ballou and Gordon Ford at the University of Michigan as previously described (Brisette et al., 1989). Fluorescence kinetic data were collected with an On-Line Instrument Systems (OLIS) computer program (on a Zenith Z-100). All kinetic data were analyzed on personal computers with the program Fit-87 written by Dr. Christopher Batie at the University of Michigan. Rapid-scanning stopped-flow studies were conducted with an apparatus built by L. David Arscott at the VA Medical Center (Ann Arbor, MI) and equipped with a Tracor-Northern Model 6500 detector with a 512-element photodiode array. Samples were made anaerobic by several cycles of evacuation followed by flushing with either nitrogen or argon passed through an R & D oxygen trap (R & D Separations) and an Oxisorb (Messer Griesheim) indicator column.

Construction of pMDO5. The construction of pMDO5 was accomplished in a two-step procedure as summarized in Figure 1. Briefly, the 1748-bp *Hin*dIII/*Sal*I fragment from pKAM1 was ligated with pMMa558a559 that had been previously digested with *Hin*dIII and *Sal*I and treated with calf intestinal phosphatase. The resulting plasmid was analyzed by restriction digestion with *Aha*II, *Eco*RI, *Hin*dIII, and *Sal*I. The presence of the Ala_{135} and Ala_{140} mutations was confirmed by double-stranded Sanger sequencing with AMV reverse transcriptase (Seidman, 1985) using the oligonucleotide 5′-TTACTGCGGTCAATCGTA-3′ (Moore, 1989) as a sequencing primer. The resulting plasmid carrying the ACAA mutant *merA* gene along with the remainder of the *mer* operon is designated pMM4302.

To express the ACAA mutant protein, pMM4302 was digested with *Aha*II, the 1861-bp *merA*-containing fragment isolated, and ligated with pSE181 previously treated with *Cla*I and calf intestinal phosphatase (Moore & Walsh, 1989). Ampicillin-resistant transformants were analyzed by digestion with *Eco*RI. Protein expression was confirmed by SDS–PAGE (Laemmli, 1970) of crude extract prepared by sonication of cells induced with IPTG (Amann et al., 1983). The overproduction plasmid pMDO5 expresses the ACAA mutant protein.

Protein Purification. The ACAA and $Ala_{10}Ala_{13}$ mutant proteins were purified from *E. coli* JM105 or W3110 *lacI*^{q} harboring pMDO5 or pMMOa10a13. Protein purification was performed as previously described (Schultz et al., 1985; Miller et al., 1989).

Results

Spectral Characteristics of the Mercuric Reductase ACAA Mutant. Previous studies with wild-type mercuric reductase and site-directed mutants have shown that the long-wavelength absorption of the two electron reduced enzyme is due to a charge-transfer interaction between oxidized flavin as acceptor and the thiolate anion of Cys_{140} as donor (Schulz et al., 1985). These spectral properties of the EH_2 form of mercuric reductase (Fox & Walsh, 1982, 1983) are quite analogous to those of glutathione reductase and lipoamide dehydrogenase, which also possess long-wavelength charge-transfer absorption bands, due in each case to interaction of the oxidized flavin with the active site thiol residue further removed from the N-terminus (Williams, 1976; Arscott et al., 1981). In previous work it has been shown that, in addition to the active site residues in mercuric reductase, Cys_{135} and Cys_{140}, the two residues Cys_{558} and Cys_{559} must be in the reduced form for efficient catalysis of Hg(II) reduction (Miller et al., 1989). The triple mutant enzyme, ACAA, in which Cys_{135}, Cys_{558}, and Cys_{559} have been changed to alanine residues, leaving only Cys_{140} of the active site cysteines intact, is thus devoid of Hg(II) reductase activity; nevertheless, it still retains a pronounced charge-transfer absorption (at pH 9.8, λ_{max} of 338, 430, and 550 nm; ϵ = 8.4, 8.6, and 2.6 mM^{-1} cm^{-1}, respectively). As the pH is lowered, there is a progressive loss of the long-wavelength band and an increase in absorbance in the 430–490-nm region, as shown in Figure 2. At pH 4.9 the spectrum is typical of an oxidized flavoprotein, with λ_{max} = 360 and 446 nm and ϵ = 8.4 and 11.3 mM^{-1} cm^{-1}.

The enzyme at high pH has only weak fluorescence, which increases progressively as the pH is decreased, to reach a value at pH 4.9 that is 5-fold greater than that of free FAD. Throughout the whole pH range, the fluorescence excitation spectrum retains the same shape, similar to that of the absorption spectrum at pH 4.9 with excitation maxima at 360 and 446 nm (Figure 2), suggesting that the fluorescence derives from a single flavin species. The fluorescence intensity and the absorbance at 560 nm as a function of pH are shown in the inset to Figure 2 and are freely reversible by adjusting the pH in either direction. Both show a pK_a of 6.66, which may reasonably be ascribed to the ionization of Cys_{140}.

Formation of a Flavin C(4a)–Thiol Adduct at pH 4.9 Induced by Binding of NADP$^+$. At low pH values, the mercuric reductase ACAA mutant exhibits dramatic changes in its absorption spectrum on titration with $NADP^+$, as shown in Figure 3. Loss of the typical oxidized flavin absorption is accompanied by the nearly isosbestic formation of a species with λ_{max} = 382 nm, ϵ = 7.5 mM^{-1} cm^{-1}. From the absorption

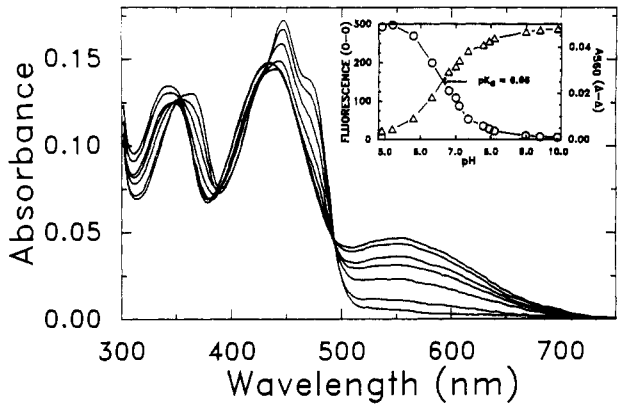

FIGURE 2: pH titration of mercuric reductase ACAA mutant enzyme in 0.05 M potassium phosphate buffer, pH 7.3, containing 0.3 mM EDTA. The pH was adjusted by addition of a few grains of powdered citric acid, and the pH and absorption and fluorescence spectra were recorded. The sample was maintained at 0–4 °C throughout the titration and was filtered through the same 0.45-μm filter (Acro LC13, Gelman Sciences) after each pH adjustment. After the lowest pH was reached, the pH was raised by the addition of finely powdered potassium carbonate, up to a pH value of 9.8. Selected spectra are shown. These can be identified by the progressive decrease in the long-wavelength absorbance; spectra are recorded at pH 9.05, 7.95, 7.3, 7.0, 6.4, 5.9, and 5.1. The inset shows the A_{560} as a function of pH, as well as the fluorescence intensity measured with excitation at 446 nm and emission at 525 nm.

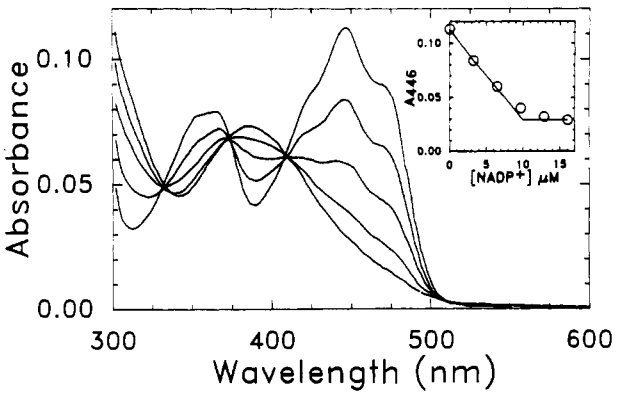

FIGURE 3: Formation of a flavin C(4a)–cysteinyl adduct at pH 4.9 induced by binding of NADP+. Mercuric reductase ACAA mutant enzyme (10.0 μM) was dissolved in 0.1 M sodium acetate buffer, pH 4.9, and titrated with NADP+ at 4 °C. Spectra with decreasing absorbance at 446 nm were recorded before addition and after 3.26, 6.49, 9.70, and 16.1 μM NADP+. The inset shows a plot of A_{446} vs the concentration of NADP+.

changes at 446 nm, which are nearly stoichiometric with the NADP+ added, a K_d of ≈0.13 μM can be calculated by assuming the process is a simple binding equilibrium. However, the changes are also accompanied by a loss of the enzyme fluorescence to a final level of ca. 6% of the starting fluorescence. For a simple binding equilibrium with a K_d of 0.13 μM, only 2% of the initial fluorescence should remain at the end point of the experiment in Figure 3. These results suggest that formation of the species absorbing at 382 nm involves a two-step process, as shown in eq 1, where the in-

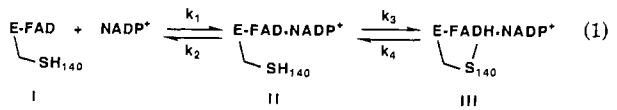

(1)

termediate formed upon binding of NADP+ (species II) also has some fluorescence. Thus, the residual fluorescence remaining in the presence of a saturating concentration of NADP+ provides a measure of the equilibrium between the intermediate (II) and the final complex (III) that absorbs at

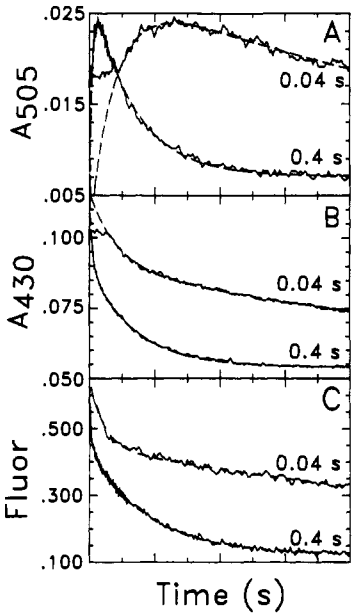

FIGURE 4: Stopped-flow traces for NADP+ binding-induced changes at pH 4.9. (Panels A and B) Traces obtained upon mixing ACAA mutant enzyme (5.5 μM after mixing) with NADP+ (50 μM after mixing) at pH 4.9, 4 °C. Absorbance changes at 505 (panel A) and 430 nm (panel B) are shown for time frames of 0.04 and 0.4 s. The solid lines are data, and the dashed lines are biphasic fits to the data with rate constants of ca. 250 and 16 s^{-1}. (Panel C) Fluorescence changes upon mixing ACAA mutant enzyme (0.5 μM after mixing) with NADP+ (50 μM after mixing) in a stopped-flow instrument at pH 4.9, 4 °C, with λ_{ex} = 446 nm and a Schott OG 515 long-wavelength pass filter (515 nm and longer transmits) placed in the emission path. The solid lines are data, and the dashed line is a biphasic fit with rate constants of ca. 450 and 11.5 s^{-1}.

382 nm and depends on the fluorescence intensity of the intermediate (II) relative to that of the starting enzyme (I). Further evidence for this proposal is provided by the kinetic studies described below.

The absorption spectrum of the final product is completely consistent with those previously assigned to flavin C(4a)-adducts (Ghisla et al., 1974, 1977; Kemal et al., 1977; Vervoort et al., 1986) and is similar to that calculated from the spectral changes associated with binding of NAD+ to lipoamide dehydrogenase in which the interchange thiol Cys_{46} of the active site dithiol ($Cys_{46}Cys_{51}$) had been alkylated by iodoacetamide (Thorpe & Williams, 1981) and to that transiently observed on reduction of wild-type mercuric reductase at low pH (Sahlman et al., 1986). However, in distinction to the latter two results, where only a portion of the FAD of the dimeric enzymes was converted to the C(4a)-adduct, the present results indicate almost complete conversion of the enzyme to the C(4a)-adduct. As shown below, formation of the C(4a)-adduct is freely reversible and dependent on both pH and NADP+ concentration.

Kinetics of Formation of the Flavin C(4a)–Thiol Adduct in the ACAA Mutant. The rate of formation of the flavin C(4a)-adduct was followed both by absorbance and by fluorescence at pH 4.9, 4 °C, as a function of NADP+ concentration. Representative traces are shown in Figure 4 for the absorbance at two wavelengths (panels A and B) and for the fluorescence (panel C). The reaction is distinctly biphasic, with a rapid increase in absorbance followed by a slower decrease in the range 480–510 nm and a rapid decrease followed by a slower decrease in the range 420–480 nm. In the range 375–390 nm, the faster phase is essentially absent, but there is a rise in the absorbance at a rate consistent with that of the slower phase seen at the other wavelengths (data not shown).

Table I: Fluorescence Kinetic Data for Formation of the C(4a)-Adduct in the ACAA Mutant[a]

$NADP^+$ (μM)	k_{slow} (s^{-1})	k_{fast} (s^{-1})
2.2	8.17 ± 0.13	138 ± 19
3.2	9.24 ± 0.20	155 ± 17
4.3	9.82 ± 0.28	167 ± 23
6.1	10.35 ± 0.10	215 ± 43
10.2	10.90 ± 0.18	273 ± 34
24.9	11.50 ± 0.27	360 ± 80
49.5	11.58 ± 0.34	555 ± 220

[a] Reaction conditions were 0.5 μM final enzyme concentration, 100 mM sodium acetate, pH 4.9, and $T = 4$ °C. The reaction was followed by the decrease of flavin fluorescence (cf. Figure 4C).

The fluorescence data also show a rapid decrease followed by a slower decrease to a low residual level of fluorescence. This biphasic decrease in the fluorescence is completely consistent with the hypothesis of eq 1, where it is proposed that an intermediate is formed that retains a significant amount of fluorescence.

The absorbance data obtained with 5.5 μM enzyme and a range of 25–113 μM $NADP^+$ (final concentrations after mixing) allowed us to estimate a K_d of ≈4 μM for the oxidized enzyme–$NADP^+$ complex. However, this value is well below the lowest concentration of $NADP^+$ (25 μM) that could be used with 5.5 μM enzyme to obtain pseudo-first-order kinetics. Hence, we employed fluorescence stopped-flow techniques to examine the concentration dependence of both phases using 0.5 μM final enzyme concentration and $NADP^+$ concentrations ranging from 2 to 50 μM as summarized in Table I.

From the data in Table I, it can be seen that the minimal value observed for k_{fast} (138 s^{-1} at 2.2 μM) is an order of magnitude greater than the maximal value for k_{slow} (11.6 s^{-1} at 49.5 μM), indicating that the two steps of eq 1 are well separated and can be analyzed separately with little introduction of error. The fast phase was only well determined when very low concentrations of $NADP^+$ were used. The observed rate constants show a linear dependence on the $NADP^+$ concentration with a non-zero intercept value, indicating that this phase is due to the binding of $NADP^+$ to the oxidized enzyme in an equilibrium step as shown in eq 1. Analysis of the data in Table I (using only the lowest five concentrations where the amplitudes of the changes were more significant and the estimated errors smaller) gives a limiting first-order dissociation rate constant (k_2) of ca. 100 ± 25 s^{-1} and a second-order association rate constant (k_1) of ca. 1.7 × 10^7 M^{-1} s^{-1}; the ratio of these gives a K_d for $NADP^+$ of ca. 5.7 μM. Results of a second experiment gave $k_2 \approx 55$ s^{-1}, $k_1 \approx 2.2 \times 10^7$ M^{-1} s^{-1}, and $K_d \approx 2.5$ μM (data not shown). These values should be regarded as only approximate, owing to the small amplitudes of the fast phase and the difficulty of determining the rates, particularly at the higher concentrations of $NADP^+$, where most of the fluorescence changes associated with the fast phase occurred in the dead time of the stopped-flow apparatus.

The slow phase of the reaction is well resolved from the fast phase and is well determined. The observed rate constant shows a hyperbolic dependence on the $NADP^+$ concentration, consistent with this step being the second step of the two-step process (eq 1) involving formation of an oxidized enzyme–$NADP^+$ complex (II) followed by the chemical reaction to form the C(4a)-adduct (III). Thus, double-reciprocal plots of $1/k_{obs}$ vs $1/[NADP^+]$ are linear. Strickland et al. (1975) have analyzed the behavior of two-step reversible reactions such as that in eq 1 and have shown that $1/k_{slow}$ for the formation of III in eq 1 vs $1/[NADP^+]$ should be nonlinear. However, significant curvature does not arise until the concentration of substrate ($NADP^+$ in this case) is well below the K_d. Due to experimental limitations, the lowest concentration of $NADP^+$ used in these experiments was in the range of the K_d estimated above rather than far below K_d. Hence, all of the $1/k_{slow}$ values are in the near-linear portion of the double-reciprocal plot. From the double-reciprocal analysis of the fully reversible system, 1/intercept = $k_3 + k_4$, and by use of the maximal slope at high substrate, slope/intercept ≈ $K_d \approx k_2/k_1$ (Strickland et al., 1975). Such analysis of the experiments in Table I gives a value of 12 s^{-1} for $k_3 + k_4$ and a value of $K_d \approx 1.0$ μM. Analysis of a second experiment (data not shown) gives $k_3 + k_4 = 12$ s^{-1} and $K_d \approx 1.4$ μM. These values are in reasonably good agreement with the values for K_d of 5.7 and 2.5 μM estimated in the analysis of the fast phase, considering the large error in the measurement of the fast phase (largely due to the magnitude of the rate constant and the low K_d). The average of the four values determined from the kinetics gives an estimate of 2.65 ± 1.8 μM for the K_d of the oxidized enzyme–$NADP^+$ complex. Solution for the separate values of k_3 and k_4 is given below.

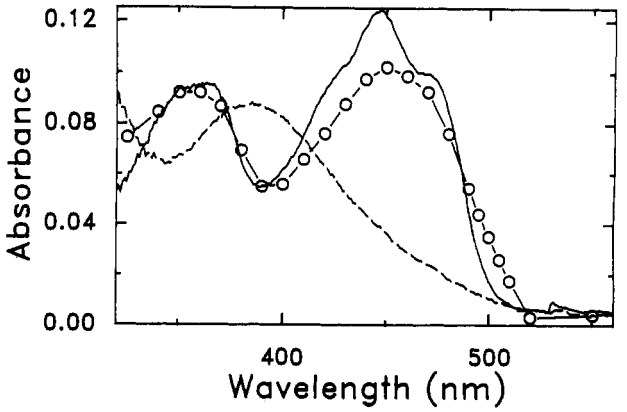

FIGURE 5: Absorption spectra obtained during the reaction of mercuric reductase ACAA mutant at pH 4.9, 4 °C, with $NADP^+$. The spectra were obtained with the stopped-flow instrument during experiments such as shown in Figure 4. Solid curve, enzyme (5.5 μM after mixing) in 0.1 M acetate, pH 4.9, mixed with an equal volume of buffer to give the spectrum of unreacted enzyme. Circles, spectrum of the oxidized enzyme–$NADP^+$ complex calculated from the absorbance at 10 ms after mixing enzyme with a final concentration of 50 μM $NADP^+$. Broken line, spectrum of the flavin C(4a) reaction product recorded after 10 s.

Since the kinetic results are consistent with the hypothesis in eq 1, the spectral changes occurring in the fast phase of the reaction (k_1, k_2) should represent the rapid equilibrium formation of the oxidized enzyme–$NADP^+$ complex (II). The absorption spectrum of the reaction mixture at the end of the fast phase (10 ms) is shown in Figure 5 (O—O). From the kinetics, it is estimated that ca. 90% of the intermediate should be present at this point. This spectrum nicely confirms the postulated nature of the intermediate as it is essentially identical with the typical spectrum of $NADP^+$ complexes of oxidized wild-type mercuric reductase (Sahlman et al., 1984) and of all mutant forms of the enzyme lacking a thiolate–flavin charge-transfer interaction (unpublished results).

The retention of some of the enzyme–FAD fluorescence in the primary E_{ox}–$NADP^+$ complex (II; eq 1) is also consistent with the properties of the same complex in both wild-type enzyme and other mutants of the enzyme. Extrapolation of the slow-phase fluorescence changes of the reaction to time zero should yield the fluorescence of the intermediate. In the reaction of enzyme with a near-saturating concentration of $NADP^+$ (50 μM), a value of 49% of the initial fluorescence was obtained by extrapolation. With an estimated K_d for

$NADP^+$ of 2.65 μM, the enzyme should be ca. 95% saturated under these conditions. Correcting for the fluorescence of the remaining E_{ox} (5%) gives a fluorescence for the intermediate of 46% that of the unliganded enzyme. This again is consistent with wild-type enzyme where the E_{ox}–$NADP^+$ complex has ca. 45% of the fluorescence of the unliganded enzyme (Miller and Massey, unpublished observation).

Determination of the fluorescence intensity of the E_{ox}–$NADP^+$ Michaelis complex now allows for calculation of the equilibrium constant between the Michaelis complex and the flavin C(4a)-adduct ($K_{eq} = k_3/k_4$, eq 1). By use of the two-step equilibrium described in eq 1 with $k_2/k_1 = 2.65$ μM and the residual fluorescence under conditions of the titration in Figure 3, the best estimate for K_{eq} is 13. With this determination of K_{eq}, we now have two equations by which we can evaluate k_3 and k_4: $K_{eq} = k_3/k_4 = 13$ and from the kinetic analysis $k_{slow} = k_3 + k_4 = 12$ s^{-1}. Solution of these two equations gives $k_3 = 11.1$ s^{-1} and $k_4 = 0.9$ s^{-1}. An independent estimation of K_{eq} can be made by comparison of the overall K_d (k_2k_4/k_1k_3) of 0.13 μM determined by the equilibrium titration of Figure 3 with the kinetically determined value of the primary binding step (k_2/k_1) discussed above (2.65 μM). From these measurements, K_{eq} can be estimated as ca. 20, in fairly good agreement with the value obtained from the fluorescence of the final equilibration mixture.

One discrepancy in the kinetics should be noted. When the slow phase was characterized by fluorescence, the extrapolated value obtained in both experiments was 12.0 ± 0.5 s^{-1}. In contrast, in the absorbance mode, the observed rate with 50 μM $NADP^+$ was 15.5 ± 1.5 s^{-1}, and the extrapolated value was ca. 16.5 s^{-1}. However, careful examination of several of the traces obtained at different wavelengths suggests that the slow phase may be better fit by two exponentials with rate constants that are only marginally different. This suggests to us that perhaps the two subunits of the dimer react at slightly different rates to give the C(4a)-adduct and that the difference in the rates observed by absorbance vs fluorescence may indicate a difference in the spectral properties of the two monomers. Many such differences in the behavior of the two monomers of the dimeric mercuric reductase have been observed by us and will be reported elsewhere (unpublished results).

Kinetics of Formation of the Flavin C(4a)–Thiol Adduct in a Wild-Type Mimic, the $Ala_{10}Ala_{13}$ Mutant. It was previously reported that reduction of the wild-type enzyme with NADPH at pH 5.1 results in the rapid formation of 50–70% of an intermediate species with an extrapolated spectrum essentially identical with that of the C(4a)-adduct described here (Sahlman et al., 1986). This intermediate then decays to other species with spectra that were not well described; hence, it was uncertain to what extent the C(4a)-adduct is stabilized in the wild-type enzyme under these conditions. It was germane to the studies on the ACAA mutant to test whether with wild-type enzyme a flavin C(4a)-adduct could be detected in the reverse direction and, if so, whether its rate of formation was consistent with that for the ACAA enzyme. Thus, we have also examined the reaction of the EH_2 form of the $Ala_{10}Ala_{13}$ mutant mercuric reductase with $NADP^+$ at pH 5.1, using a stopped-flow instrument equipped with a rapid-scanning diode array detector [$Ala_{10}Ala_{13}$ is a wild-type equivalent in terms of Hg(II) reductase activity (Miller et al., 1989)]. As summarized in Figure 6, the enzyme rapidly binds $NADP^+$ (in the dead time of the instrument) to give a mixture of the protonated (Cys_{140}–SH) and deprotonated (Cys_{140}–S^-) EH_2–$NADP^+$ Michaelis complexes (dashed-line spectrum)

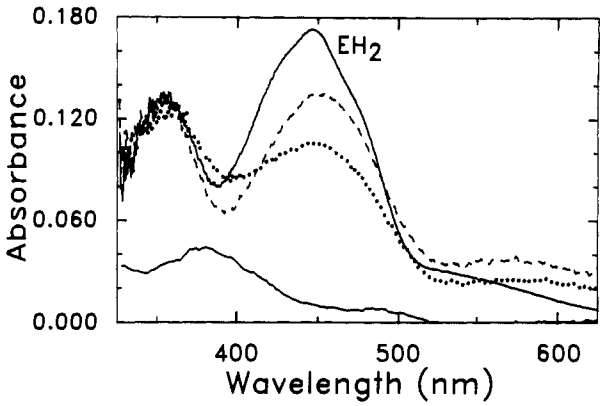

FIGURE 6: Partial formation of the flavin C(4a)–thiol adduct in the EH_2–$NADP^+$ complex of $Ala_{10}Ala_{13}$ mercuric ion reductase at pH 5.1. $Ala_{10}Ala_{13}$ enzyme (20.9 μM) was titrated with dithionite (anaerobically) to the two electron reduced form (EH_2) and was mixed in a stopped-flow spectrophotometer with 10 equiv of $NADP^+$ at pH 5.1, 4 °C. Selected spectra, recorded on a Tracor Northern rapid-scanning instrument with a diode array detector (Model 6500), include EH_2 mixed with buffer (as labeled) and EH_2 mixed with $NADP^+$ (10.5 and 105 μM, respectively, after mixing) at 4.5 (– –) and at 362 ms (···). The lower solid-line spectrum is that of the C(4a)-adduct component of the equilibrium mixture and was obtained by subtracting 70% of the dead-time spectrum (– –) from the final spectrum (···).

having some of the long-wavelength charge-transfer band typical of the deprotonated complex. Then, as evidenced by the decrease in absorbance at wavelengths of >415 nm and the increase in absorbance in the region 380–415 nm, the enzyme equilibrates to give a final mixture (dotted-line spectrum) of the protonated and deprotonated complexes and the flavin C(4a)–thiol adduct. Since the final mixture retains ca. 70% of the absorbance at long wavelength, 70% of the dead-time spectrum was subtracted from the final spectrum to obtain the spectrum of the C(4a)-adduct in the mixture (lower solid line). This species has a $\lambda_{max} \approx 380$ nm and an $\epsilon \approx 7$ mM^{-1} cm^{-1}, consistent with the properties of the flavin C(4a)-adduct in the ACAA mutant ($\epsilon \approx 7.5$ mM^{-1} cm^{-1}). At the concentration of $NADP^+$ used in this experiment (105 μM), the rate of formation of the C(4a)-adduct from the Michaelis complex was calculated to be ca. 17 s^{-1}, in good agreement with the values obtained with the ACAA mutant (12–16 s^{-1}). Thus, the C(4a)-adduct on the ACAA mutant is likely to be a relevant species in catalysis.

Kinetic Competence of the C(4a)-Adduct in the $Ala_{10}Ala_{13}$ Mutant. If the C(4a)-adduct is an intermediate in the normal Hg(II) reduction catalyzed by mercuric reductase, it must break down to the EH_2 form of the enzyme at a rate at least as fast as turnover. From the above experiments with the ACAA mutant, this rate (k_4 in eq 1) was estimated to be ca. 0.9 s^{-1}. For comparison with this, we have determined the rate of Hg(II) reduction under anaerobic conditions in 75 mM sodium acetate buffer containing 0.3 mM EDTA at pH 5.1 and 5 °C. In the presence of 100 μM NADPH, 100 μM $HgCl_2$, 1 mM 2-mercaptoethanol, and 5 μM $Ala_{10}Ala_{13}$ mercuric reductase, the rate of turnover was determined to be 0.01–0.03 s^{-1} with different preparations of enzyme. These results clearly show that the rate of breakdown of the C-(4a)-adduct reported above is sufficiently fast to account for the rate of the normal catalytic reduction of Hg(II) at this pH and thereby confirm the viability of the C(4a)-adduct as a possible intermediate in catalysis. It has previously been shown that the C(4a)-adduct is an intermediate in the reduction of wild-type mercuric reductase E_{ox} to EH_2 at this pH (Sahlman et al., 1986); this reaction constitutes the priming event of normal catalysis (Miller et al., 1986, 1989; Sandstrom

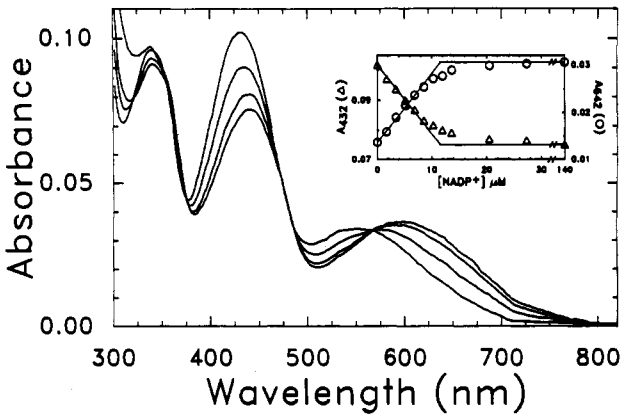

FIGURE 7: Spectral changes on binding $NADP^+$ to mercuric reductase ACAA mutant enzyme at pH 9.2. ACAA enzyme (11.6 μM) was dissolved in 42 mM sodium bicarbonate/17 mM potassium phosphate buffer, pH 9.2, and titrated with $NADP^+$ at 4 °C. Selected spectra are shown, in order of decreasing A_{432}, for 0, 5.12, 11.94, and 139.8 μM $NADP^+$. The inset shows plots of A_{432} (Δ) and A_{642} (O) as a function of $NADP^+$ concentration.

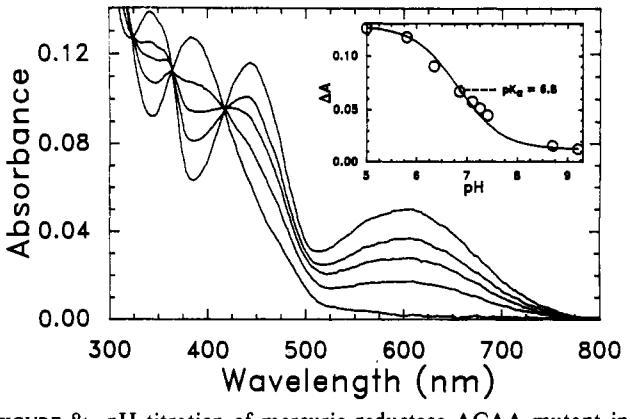

FIGURE 8: pH titration of mercuric reductase ACAA mutant in complex with $NADP^+$. The enzyme (17.3 μM), dissolved in the same buffer as in Figure 7 and mixed with 83 μM $NADP^+$, was treated with powdered citric acid in the same way as described in the legend to Figure 2. Selected spectra are shown: the five spectra with decreasing A_{600} were at pH values of 9.2, 7.4, 6.85, 6.35, and 4.95. The inset shows the difference in absorbance at 384 and 600 nm as a function of pH, yielding a pK_a of 6.8.

& Lindskog, 1988). During turnover, however, the enzyme remains in the EH_2 form, undergoing the reaction

$$EH_2\text{–NADPH–Hg(II)} \rightarrow EH_2\text{–}NADP^+ + Hg(0)$$

It has been proposed that NADPH first reduces the flavin, which then reduces Hg(II) by one of several possible mechanisms including direct electron transfer or formation of either a C(4a)–thiol adduct or a C(4a)–Hg(II) adduct (Miller et al., 1989). The above results indicate that a C(4a)–thiol adduct is at least a kinetically competent intermediate.

Binding of $NADP^+$ at pH 9.2 and pH Titration of the Oxidized Enzyme–$NADP^+$ Complex. The binding of $NADP^+$ is very tight to all species of mercuric reductase that have been studied and results in pronounced changes in absorption spectra. The spectral changes accompanying the formation of the ACAA enzyme–$NADP^+$ complex at pH 9.2 are shown in Figure 7. There is a decrease in the intensity of the 430-nm band and a small shift in λ_{max} to 440 nm; at the same time the 550-nm band is shifted to 600 nm, with a small increase in extinction. These changes are most reasonably ascribed to a subtle change in the charge-transfer interaction between the flavin and Cys_{140} [which is presumably on the *si* side of the flavin by analogy to the structure of glutathione reductase (Pai & Schulz, 1983)] resulting from the binding of $NADP^+$ [which is one the *re* side of the flavin (Manstein et al., 1986)]. From an analysis of the spectral changes as a function of $NADP^+$ concentration, a K_d of 0.34–0.44 μM was calculated.

When the pH of a sample of the ACAA enzyme–$NADP^+$ complex was lowered, there was a progressive loss of the 600-nm band while the absorbance in the 380-nm region increased (Figure 8). At pH 4.95, the final species produced was clearly the C(4a)-adduct, as in the results of Figure 3. The inset of Figure 8 shows the spectral changes as a function of pH, revealing a pK_a of 6.8, almost the same as had been found for titration of the enzyme in the absence of $NADP^+$. However, the kinetics experiments at pH 4.9 described above clearly show that the Michaelis complex of *protonated* enzyme with $NADP^+$ is an intermediate on the pathway to the C-(4a)-adduct. (The reaction is seen only at low pH.) Hence, the pK_a of 6.8 represents an apparent pK_a for the two-step process (eq 2) of protonation of Cys_{140} followed by formation

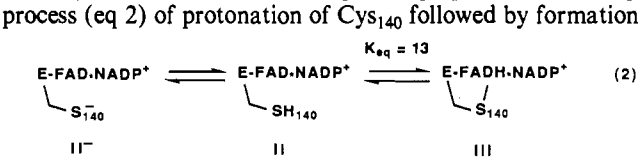

of the C(4a)-adduct. Calculation of the true pK_a of the E_{ox}–$NADP^+$ complex therefore relies on the estimation of the equilibrium constant, K_{eq}, between the protonated complex and the C(4a)-adduct, which is 13 ($pK_{eq} = -1.1$) as calculated above. The true pK_a = apparent $pK_a + pK_{eq} = 5.7$. These results demonstrate that accumulation of the flavin C(4a)–thiol adduct is dependent on both pH and the binding of $NADP^+$ as summarized in Scheme III, where the species in eq 2 correspond in order to species II^-, II, and III.

Rate of Breakdown of the C(4a)-Adduct As Measured in a pH-Jump Experiment. The behavior of the ACAA enzyme–$NADP^+$ complex as a function of pH (described by eq 2) provides us with a possible means of measuring the rate of breakdown of the C(4a)-adduct, which is the rate most pertinent to catalysis. Thus, if the C(4a)-adduct (III in Scheme III) is subjected to a rapid increase in pH to well above the pK_a, it will break down, giving the deprotonated Michaelis complex (II^- in Scheme III) as the final product. In the event that the flavin N(5)H is protected from the solvent, such a breakdown should occur via the protonated Michaelis complex (II) and, hence, would be expected to proceed at the rate of 0.9 s^{-1} estimated above from the kinetics of C(4a)-adduct formation and K_{eq}. However, if the flavin N(5)H is accessible to solvent, breakdown to the deprotonated Michaelis complex (II^- in Scheme III) could occur via deprotonation to give the highly unstable N(5)-anionic C(4a)-adduct (III^- in Scheme III) as a transient intermediate or the transition state of the reaction. To test these hypotheses, the ACAA enzyme (24 μM) was dissolved in 20 mM sodium acetate buffer, pH 4.9, in the presence of $NADP^+$ (50 μM) and was rapidly mixed in the stopped-flow spectrophotometer with an equal volume of 100 mM sodium bicarbonate, pH 9.8 (final pH 9.5). The kinetics followed at three wavelengths showed a rapid conversion of the C(4a)-adduct (III) to the deprotonated Michaelis complex (II^-) with a rate constant of 420 ± 120 s^{-1} (data not shown). This rate is clearly much faster than the 0.9 s^{-1} calculated for the breakdown of the C(4a)-adduct (III) to the protonated Michaelis complex (II), indicating that species II is not an intermediate in the breakdown at high pH. Thus, the flavin N(5)H or a nearby base must be accessible to solvent, allowing breakdown to occur via the alternative path in Scheme III ($III \rightarrow III^- \rightarrow II^-$) with the highly unstable N(5)-anionic C(4a)-adduct (III^-) as an intermediate or transition state. A mechanism involving base catalysis is

Scheme III: Equilibrium Formation of the C(4a)–Thiol Adduct in the ACAA Mutant[a]

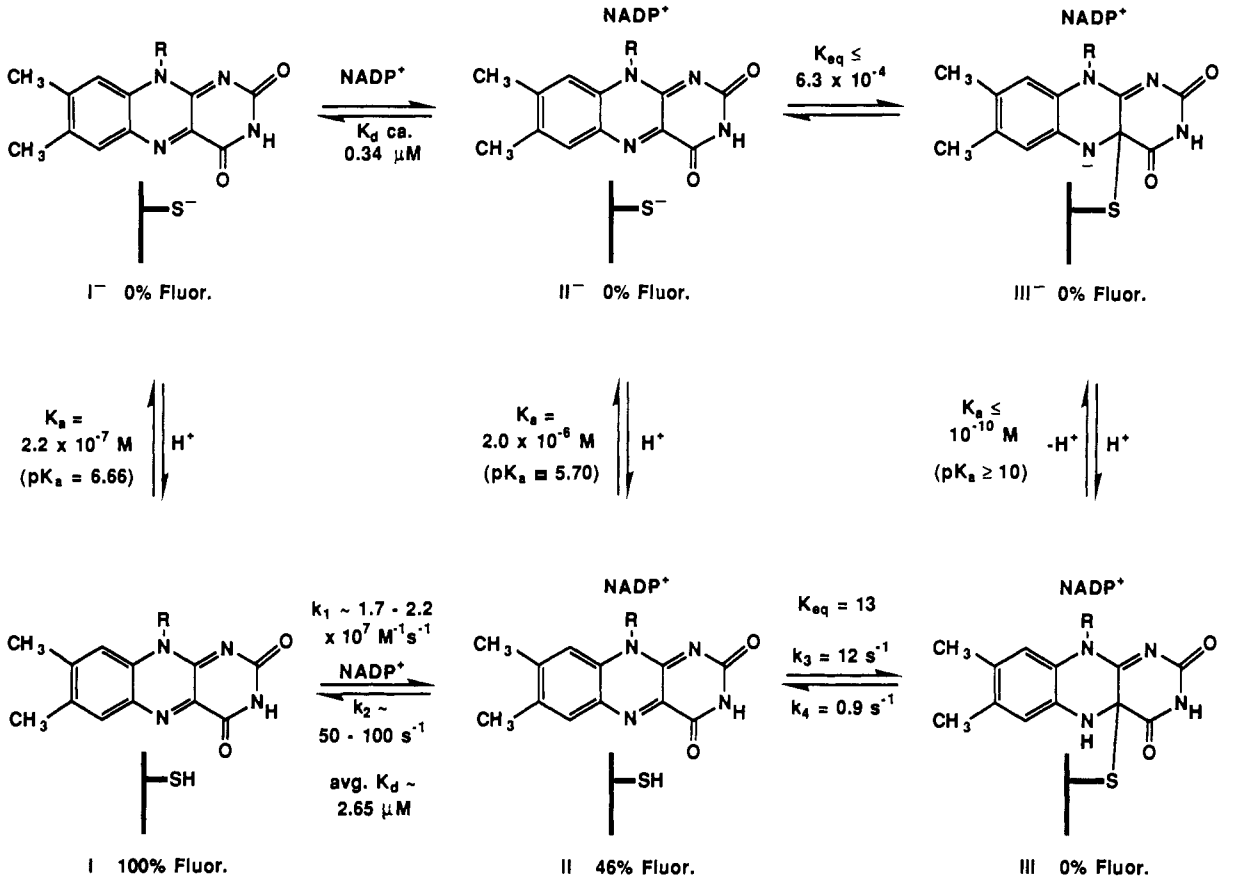

[a] K_a refers to the acid dissociation constant at each step, and Fluor is the fluorescence of each species relative to that of the unliganded enzyme at pH 4.9.

Scheme IV: Routes of Formation of Flavin C(4a)–Thiol Adduct

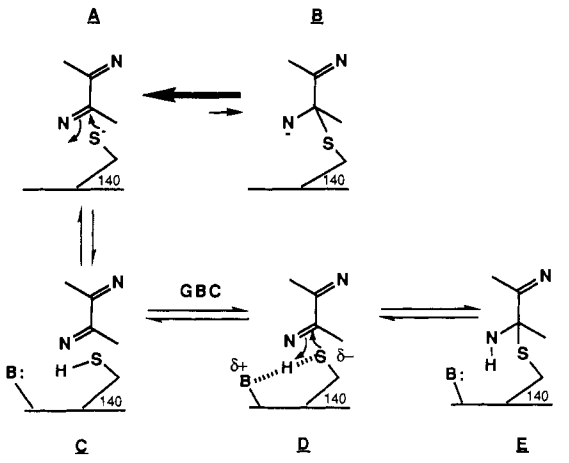

presented in Scheme IV (steps E → C).

Reaction of Mercuric Reductase ACAA Mutant at pH 4.9 with NADPH. Since the ACAA mutant lacks the intact active site disulfide and auxiliary thiols of the wild-type enzyme, it is a useful form in which to study the reduction of the enzyme-bound FAD. At high pH, where the Cys_{140} thiolate participates in a charge-transfer interaction with the flavin, reduction of the FAD by NADPH does not occur. However, at low pH, where Cys_{140} is in the protonated thiol form, no charge-transfer interaction with FAD is present. Under these conditions because the secondary changes in absorbance associated with electron transfer to the active site disulfide and the formation of complexes between EH_2 and NADPH and NADP+ are absent, the rate of frank reduction of the enzyme flavin can be followed. These experiments were carried out under anaerobic conditions at pH 4.9, 4 °C.

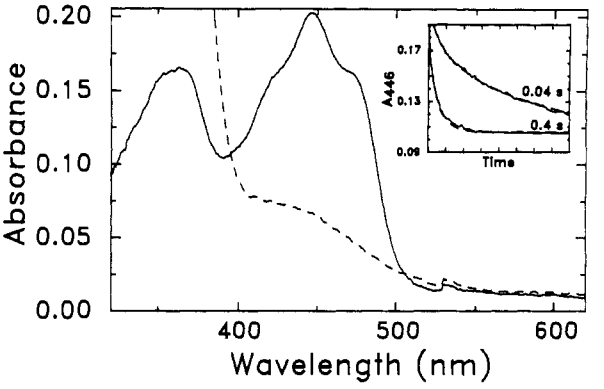

FIGURE 9: Reduction of the ACAA mutant with NADPH at pH 4.9. Oxidized ACAA mutant (9.1 μM after mixing) was mixed with 10 equiv of NADPH (91 μM after mixing) in the stopped-flow spectrophotometer at 4 °C (0.1 M acetate buffer, pH 4.9). (—) Spectrum of the starting enzyme obtained by mixing enzyme with an equal volume of buffer in the stopped-flow instrument; (– –) Spectrum taken at the end of the reaction (40 s). The inset shows a representative kinetic trace at 446 nm (—). The dashed line is a biphasic fit with rate constants of ca. 260 s^{-1} and 31 s^{-1}.

Figure 9 summarizes the spectral changes occurring upon reduction of the enzyme in the presence of 10 equiv of NADPH. A characteristic kinetic trace at 446 nm, presented in the inset, shows that reduction of the flavin is biphasic with rate constants estimated to be 260 ± 100 s^{-1} and 31.6 ± 4.3 s^{-1} and with amplitudes of −0.037 and −0.057, respectively.

There is an additional decrease at 446 nm of ca. 10% of the total change (leading to the spectrum shown in Figure 9) that occurs at a rate of 0.04 ± 0.01 s^{-1}. This final change may be due to an exchange of $NADP^+$ for NADPH on the enzyme. If we subtract the 10% of the absorbance change that occurs in the very slow phase, then the amplitude of the phase with a rate constant of 31.6 s^{-1} accounts for ca. 47% of the total amplitude change calculated from the initial and final spectra.

Under conditions identical with those of the above experiments, we found that the $Ala_{10}Ala_{13}$ enzyme undergoes a rapid bleaching of FAD concomitant with formation of the C(4a)-adduct at a rate of 190 s^{-1}, which is consistent with the observations of Sahlman et al. (1986) of a rate of 145 s^{-1} for the same process with the wild-type enzyme. Taken together, these experiments show that (a) the general behavior of the ACAA enzyme is similar to that observed for wild-type enzyme, with the distinction that ACAA is trapped at the level of reduced flavin (E–$FADH^-$, Scheme IB), and (b) the biphasic nature of the reduction of ACAA indicates that this mutant has differential reactivity of the two subunits, implying cooperativity. This is a feature of all of the mercuric reductase enzymes (unpublished results).

Discussion

The mutant form of mercuric reductase ($Ala_{135}Cys_{140}Ala_{558}Ala_{559}$; ACAA), which contains three of the four catalytically essential cysteine residues mutated to alanine residues, is devoid of NADPH–Hg(II) reductase activity. Nevertheless, it has proven to be a valuable mutant species for mechanistic studies, permitting the dissection of several aspects of the reaction mechanism that have been difficult or impossible to delineate with any of the wild-type enzymes of its class. There are two key features of the enzyme that make it valuable for these studies. First is the retention of an intact pyridine nucleotide binding site, as evidenced by the submicromolar dissociation constants reported above for the enzyme–$NADP^+$ complexes. Wild-type enzyme also exhibits very low dissociation constants for both the $NADP^+$ and NADPH complexes of EH_2 (which is the form of the enzyme the mutant best models). The second feature is the elevated pK_a of the charge-transfer thiol (Cys_{140}) relative to the pK_a of the wild-type EH_2 enzyme. Replacement of the three active site CH_2SH groups with CH_3 groups has increased the hydrophobicity of the active site and consequently has raised the pK_a of the remaining thiol nearly 2 pH units from ca. 5.0 (Sahlman and Williams, unpublished observation) to 6.7. Since the enzyme is stable at pH 5, we have been able to examine the properties of the enzyme at a pH well below the thiol pK_a, thereby eliminating the charge-transfer interaction of the thiolate with the flavin and its consequent chemical and spectral effects. Until now this has not been possible with any enzymes of the pyridine nucleotide disulfide oxidoreductase class.

As summarized in Scheme IA, it has long been considered that among this whole class of flavoproteins, reversible electron transfer between reduced pyridine nucleotide and active site disulfide proceeds via rapid reduction of the flavin by NAD(P)H to form E–$FADH^-$. This would be followed by reduction of the active site disulfide through the formation of an intermediate flavin C(4a)–thiol adduct that results from nucleophilic attack of the reduced flavin on the disulfide (Thorpe & Williams, 1981) (Scheme II). This sequence of events has, however, proved difficult to establish experimentally, since spectral characterization of the proposed flavin C(4a)-intermediate was complicated both by the rapidity of the reaction and by the complexities introduced by the presence of the several charge-transfer species (EH_2, EH_2–$NADP^+$, and EH_2–NADPH) that result from the breakdown of the postulated adduct and subsequent equilibration with the pyridine nucleotide substrate and product species present.

In the case of the mercuric reductase ACAA mutant, because there is no electrophilic active site disulfide present, reduction of the active site by NADPH should lead to accumulation of reduced flavin, because its oxidation by further electron transfer to the single thiol Cys_{140} will not occur. Similarly, in the reverse direction the C(4a)–thiol adduct will form (Scheme IB). But the absence of any other Cys–SH precludes adduct breakdown by the normal route involving nucleophilic attack of such a thiol to yield disulfide and E–$FADH^-$. Therefore the C(4a)-adduct formed in this direction will accumulate in the mutant. Hence, we have been able to monitor directly both the reduction of FAD by NADPH to form E–$FADH^-$ in the forward direction and the formation of the flavin C(4a)–thiol adduct from the reverse direction. The ACAA site-directed mutant thereby allows trapping of two species thought to be on the normal reaction pathway.

The two electron reduced form of the flavoprotein disulfide reductases consists in its stable form of primarily FAD and a thiol/thiolate pair shown as EH_2 in Scheme IA. Further reduction of the flavin by NADPH does not occur in the EH_2 forms of the wild-type mercuric reductase above the pK_a of the charge-transfer thiol. This is largely due to the lowered reduction potential of the flavin that results from the charge-transfer interaction of the electron-donating Cys_{140} thiolate with FAD and is exemplified by comparing the E_{ox}/E_{red} reduction potential for the AACC mutant mercuric reductase (which has no charge-transfer interaction), $E^{\circ\prime}_1$ = −291 mV (Distefano et al., 1989) and the EH_2/EH_4 potential for wild-type enzyme, $E^{\circ\prime}$ = −335 mV (Fox & Walsh, 1982). Likewise, reduction would not be expected to occur in the thiolate form of the ACAA enzyme [i.e., at pH values above the pK_a (6.7) of Cys_{140}]. However, at low pH in its thiol form where no charge-transfer interaction occurs, the ACAA enzyme should be a good analogue for the oxidized wild-type enzyme and, hence, should undergo reduction by NADPH. At pH 5, reduction is indeed rapid, even at 4 °C, and formation of the E–$FADH^-$ species is quantitative. This is the first time quantitative rapid reduction of flavin by NAD(P)H has been observed with a flavin disulfide oxidoreductase. Approximately half of the reduction takes place with a $t_{1/2}$ of ca. 3 ms, which is consistent with the very rapid formation of the EH_2 species in wild-type enzyme (Sahlman et al., 1984, 1986); the second half proceeds at ca. 32 s^{-1} and reflects the negative cooperativity seen in many reactions of various mutants of mercuric ion reductase (unpublished results). These results imply that the E–$FADH^-$ form of mercuric reductase is a kinetically competent intermediate to participate in the reductive half-reaction (Scheme IA).

Since transient formation of a flavin C(4a)-adduct in wild-type mercuric reductase has only been observed at low pH (Sahlman et al., 1986), it seemed likely that the adduct in the ACAA mutant may also occur at low pH. Indeed, the results of the present study show that at pH 5, after very fast formation of a Michaelis complex with $NADP^+$ (E → E–$NADP^+$, Scheme IB, eq 1), Cys_{140} is able to react relatively rapidly (≈15 s^{-1} at 4 °C) to form nearly quantitatively the adduct to the C(4a)-position of the flavin. This reaction also occurs in the wild-type enzyme at essentially the same rate, but only proceeds to ca. 30% completion, due to the much lower pK_a of the charge-transfer thiolate in the wild-type enzyme as discussed below. The accumulation of the flavin

C(4a)–S–Cys_{140} adduct in these experiments clearly shows that Cys_{140} is the nucleophile in these reactions and the conduit for passage of electrons from $FADH^-$ to the Cys_{140}–Cys_{135} disulfide in turnover with wild-type enzyme.

The requirement for $NADP^+$ binding to drive the equilibrium toward C(4a)-adduct is consistent with observations by Thorpe and Williams (1976, 1981) that formation of ca. 50% of a C(4a)–thiol adduct in a monoalkylated form of lipoamide dehydrogenase only occurs upon binding of NAD^+. One interpretation of this requirement is that binding of the positively charged $NAD(P)^+$ adjacent to the flavin increases the electrophilicity of the oxidized flavin, thereby promoting the accumulation of the C(4a)–thiol adduct when a proton is available at low pH. In the absence of a proton at high pH, the equilibrium lies in favor of the charge-transfer species (II^- in Scheme III); but here, too, the increased electrophilicity of the flavin is manifest by the lowering of the energy of the thiolate–flavin charge-transfer interaction as evidenced by the bathochromic shift in the long-wavelength band in the $NADP^+$ complex (II^-) relative to that in the unliganded enzyme (I^-) (Figure 7). Other studies on lipoamide dehydrogenase (Matthews et al., 1979) have also indicated that bound pyridine nucleotides modulate flavin–disulfide interactions.

In the reductive half-reaction, mercuric ion reductase proceeds in the direction of breakdown of the C(4a)–thiol adduct to form the dithiol and oxidized flavin (EH_2). Thus, it is necessary to determine whether the rate for conversion of III → II in Scheme III is competent for catalysis. From the fluorescence titration and kinetic studies, K_{eq} in eq 2 and in Scheme III was calculated to be ca. 13, from which the rate constant for the breakdown of the C(4a)-adduct is calculated to be 0.9 s^{-1}. From anaerobic steady-state experiments with the $Ala_{10}Ala_{13}$ (wild-type mimic) enzyme, the turnover number at pH 5.1, 4 °C, is 0.01–0.03 s^{-1}. Clearly, the breakdown of the C(4a)-adduct is fast enough to account for the normal catalysis that occurs under those conditions.

Considering that thiolates are far better nucleophiles than thiols, one might anticipate that Cys_{140}–S^- would be more likely to be the nucleophile in forming the flavin C(4a)–thiol adduct (represented in Scheme IV by species A to species B) than would its protonated form. However, it is clear from this work that the C(4a)–thiol adduct is only seen at pH values well below the pK_a of Cys_{140}–SH (pK_a = 6.66; Scheme III). This is undoubtedly due to the difficulty of forming the N(5)-anionic species B in Scheme IV, as expected from the high pK_a (ca. 20) of the N(5)H function of reduced flavin species (Venkataram & Bruice, 1984; Macheroux, Sanner, Rüterjans, Ghisla, and Müller, personal communication). A more favorable route is provided by C → D → E. Here, the thiol brings in the proton for N(5) and avoids formation of species B. It is possible that the thiol is polarized via general-base catalysis (GBC) (as depicted by D) to improve its nucleophilicity without creating an anionic nucleophile. Apparently the protonation of N(5) of the flavin is more important than creation of a thiolate nucleophile. The identity of the suggested base is not apparent from the crystal structure of the homologous glutathione reductase. The tyrosine residue in mercuric reductase occupying a position homologous with $His_{467'}$ in glutathione reductase would not be correctly positioned for this role if the tertiary structure of the two enzymes is similar in this area.

Scheme III describes the formation of the flavin C(4a)–thiol adduct and the salient protonic states involved. We have been able to measure or calculate values for all of the equilibria except the pK_a of the C(4a)-adduct. For this we have used a minimal value ($pK_a \geq 10$), well below the literature values for the pK_a (ca. 20) of the N(5)H of reduced flavin. Even with this minimal estimate for the pK_a, the anionic species III^- would never be formed to more than 1 part in 10^4; a higher pK_a would make the equilibrium between II^- and III^- lie even more in favor of II^-. In the wild-type enzyme the pK_a of the Cys_{140} thiol (5.0) is considerably lower than that in ACAA (6.7), having the same effect as raising the pH with the ACAA mutant. This shifts the equilibrium from the C(4a)-adduct (species III) toward the deprotonated Michaelis complex (II^-), thereby preventing full formation of the adduct.

The process of enhancing the breakdown of the C(4a)-adduct is favorable for normal catalysis, which proceeds in the direction of III → II^-. We are now able to address the pathway by which this conversion occurs. If the pathway was III → II → II^-, the rate of conversion of III → II should be consistent with normal catalysis, which it actually is at pH 5.0. However, this step should be pH independent, suggesting that maximum turnover rates at all pH values should be ≤0.9 s^{-1} at 4 °C. However, rates of formation of the EH_2–$NADP^+$ species with wild-type enzymes (Scheme IA) are much greater than 0.9 s^{-1} at higher pH, suggesting that the actual sequence is III → III^- → II^-. Our results provide strong experimental support for this pathway, since the pH-jump experiment with the ACAA mutant shows conversion of III → II^- at a rate of 420 s^{-1} at pH 9.5, 4 °C.

References

Amann, E., Brosius, J., & Ptashne, M. (1983) *Gene 25*, 167–178.

Arscott, L. D., Thorpe, C., & Williams, C. H., Jr. (1981) *Biochemistry 20*, 1513–1520.

Beaty, N. B., & Ballou, D. P. (1981) *J. Biol. Chem. 256*, 4611.

Brisette, P., Ballou, D. P., & Massey, V. (1989) *Anal. Biochem. 181*, 234–238.

Brown, N. L., Ford, S. J., Pridmore, R. D., & Fritzinger, D. C. (1983) *Biochemistry 22*, 4089–4095.

Bulger, J. E., & Brandt, K. G. (1971) *J. Biol. Chem. 246*, 5578–5587.

Distefano, M. D., Au, K. G., & Walsh, C. T. (1989) *Biochemistry 28*, 1168–1183.

Fox, B., & Walsh, C. T. (1982) *J. Biol. Chem. 257*, 2498–2503.

Fox, B. S., & Walsh, C. T. (1983) *Biochemistry 22*, 4082–4088.

Ghisla, S., & Massey, V. (1980) *J. Biol. Chem. 255*, 5688–5696.

Ghisla, S., Massey, V., Lhoste, L. M., & Mayhew, S. G. (1974) *Biochemistry 13*, 589–597.

Ghisla, S., Entsch, B., Massey, V., & Husain, M. (1977) *Eur. J. Biochem. 76*, 139–148.

Hamilton, G. A. (1971) in *Progress in Bioorganic Chemistry* (Kaiser, E. T., & Kezdy, F. J., Eds.) Vol. 1, pp 1–87, Wiley-Interscience, New York.

Hemmerich, P. (1968) *Proc. R. Soc. London, A 302*, 335–350.

Hevesi, L., & Bruice, T. C. (1973) *Biochemistry 12*, 290–297.

Huber, P. W., & Brandt, K. G. (1980) *Biochemistry 19*, 4568–4575.

Kemal, C., Chan, T. W., & Bruice, T. C. (1977) *J. Am. Chem. Soc. 99*, 7272–7286.

Laemmli, U. K. (1970) *Nature 227*, 680.

Loechler, E. L., & Hollocher, T. C. (1975) *J. Am. Chem. Soc. 97*, 3235–3237.

Maniatis, T., Fritsch, E. F., & Sambrook, J. (1982) *Molecular Cloning; a Laboratory Manual*, Cold Spring Harbor Laboratory, Cold Spring Harbor, New York.

Manstein, D. J., Pai, E. F., Schopfer, L. M., & Massey, V. (1986) *Biochemistry 25*, 6807–6816.
Massey, V., & Ghisla, S. (1974) *Ann. N.Y. Acad. Sci. 227*, 46–465.
Massey, V., Gibson, Q. H., & Veeger, C. (1960) *Biochem. J. 77*, 341–351.
Matthews, R. G., & Williams, C. H., Jr. (1976) *J. Biol. Chem. 251*, 3956–3964.
Matthews, R. G., Ballou, D. P., & Williams, C. H., Jr. (1979) *J. Biol. Chem. 254*, 4974–4981.
Miller, S. M., Ballou, D. P., Massey, V., Williams, C. H., Jr., & Walsh, C. T. (1986) *J. Biol. Chem. 261*, 2081–2084.
Miller, S. M., Moore, M. J., Massey, V., Williams, C. H., Jr., Distefano, M. D., Ballou, D. P., & Walsh, C. T. (1989) *Biochemistry 28*, 1194–1205.
Moore, M. J. (1989) Ph.D. Thesis, Department of Chemistry, Massachusetts Institute of Technology, Cambridge, MA.
Moore, M. J., & Walsh, C. T. (1989) *Biochemistry 28*, 1183–1194.
O'Donnell, M. E., & Williams, C. H., Jr. (1984) *J. Biol. Chem. 259*, 2243–2251.
Pai, E. F., & Schulz, G. E. (1983) *J. Biol. Chem. 258*, 1752–1757.
Sahlman, L., Lambeir, A.-M., Lindskog, S., & Dunford, H. B. (1984) *J. Biol. Chem. 259*, 12403–12408.
Sahlman, L., Lambeir, A., & Lindskog, S. (1986) *Eur. J. Biochem. 156*, 479–488.
Sandstrom, A., & Lindskog, S. (1988) *Eur. J. Biochem. 173*, 411–415.
Schultz, P. G., Au, K. G., & Walsh, C. T. (1985) *Biochemistry 24*, 6840–6848.
Searls, R. L., Peters, J. M., & Sanadi, D. R. (1961) *J. Biol. Chem. 236*, 2317–2322.
Seidman, M. (1985) *BMBiochemica 2* (5), 10.
Strickland, S., Palmer, G., & Massey, V. (1975) *J. Biol. Chem. 250*, 4048–4052.
Thorpe, C., & Williams, C. H., Jr. (1976) *J. Biol. Chem. 251*, 7726–7728.
Thorpe, C., & Williams, C. H., Jr. (1981) *Biochemistry 20*, 1507–1513.
Venkataram, U. V., & Bruice, T. C. (1984) *J. Am. Chem. Soc. 106*, 5703–5709.
Vervoort, J., Müller, F., Lee, J., van den Berg, W. A. M., & Moonen, C. T. W. (1986) *Biochemistry 25*, 8062–8067.
Walker, W. H., Hemmerich, P., & Massey, V. (1970) *Eur. J. Biochem. 13*, 258–266.
Williams, C. H., Jr. (1976) *Enzymes (3rd Ed.) 13*, 89–173.
Yokoe, I., & Bruice, T. C. (1975) *J. Am. Chem. Soc. 97*, 450–451.

Differential Inhibitory Effects of Some Catechin Derivatives on the Activities of Human Immunodeficiency Virus Reverse Transcriptase and Cellular Deoxyribonucleic and Ribonucleic Acid Polymerases

Hideo Nakane and Katsuhiko Ono*
Laboratory of Viral Oncology, Aichi Cancer Center Research Institute, Chikusa-ku, Nagoya 464, Japan
Received July 26, 1989; Revised Manuscript Received November 2, 1989

ABSTRACT: The two components of *Camellia sinensis* (tea plant) [i.e., (−)-epicatechin gallate and (−)-epigallocatechin gallate] were found to differentially inhibit the activities of reverse transcriptase and cellular DNA and RNA polymerases. Under the assay conditions optimized for each enzyme species, the strongest inhibition by these compounds was observed with reverse transcriptase. The concentrations of (−)-epicatechin gallate and (−)-epigallocatechin gallate required for 50% inhibition of the activity of human immunodeficiency virus (HIV) reverse transcriptase were in the range of 0.01–0.02 μg/mL. On the other hand, neither (−)-epicatechin, (−)-epigallocatechin, nor gallic acid, the constituents of (−)-epicatechin gallate and (−)-epigallocatechin gallate, was inhibitory to the activity of HIV reverse transcriptase at concentrations up to 1 μg/mL. The mode of inhibition of reverse transcriptase and other DNA polymerases by these compounds was competitive with respect to the template-primer, whereas the mode of inhibition of RNA polymerase was competitive with respect to the nucleotide substrate. The K_i values of HIV reverse transcriptase for (−)-epicatechin gallate and (−)-epigallocatechin gallate were determined to be 7.2 and 2.8 nM, respectively, which are smaller by 1–2 orders of magnitude than the K_i's of other DNA and RNA polymerases for these compounds.

Since AIDS[1] was found to be caused by a retrovirus, designated as HIV, HIV-associated reverse transcriptase has been considered to be one of the appropriate targets for chemotherapeutic approaches toward AIDS. Various reverse transcriptase inhibitors have already been reported to exert anti-HIV effects, e.g., suramin (Mitsuya et al., 1984; Broder et al., 1985), HPA23 (Rozenbaum et al., 1985), AZT (Mitsuya et al., 1985; Yarchoan et al., 1986), and DDC (Mitsuya & Broder, 1986). However, most of the antiretroviral agents that inhibit reverse transcriptase also inhibit cellular DNA polymerases. Typical examples are suramin and HPA23, which inhibit both reverse transcriptase and cellular DNA polymerases (Ono et al., 1988a,b). This explains at least part of the side effects observed upon administration of these

[1] Abbreviations: AIDS, acquired immune deficiency syndrome; ARC, AIDS-related complex; HIV, human immunodeficiency virus; RLV, Rauscher murine leukemia virus; suramin, hexasodium *N,N'*-bis[3-[[[4-methyl-3-[[(4,6,8-trisulfo-1-naphthyl)amino]carbonyl]phenyl]amino]-carbonyl]phenyl]carbamide; HPA23, hexaoctacontaoxononaantimonateheneicosatungstate(19−) heptadecaammonium salt; AZT and AZTTP, 3'-azido-3'-deoxythymidine and its 5'-triphosphate; DDC, 2',3'-dideoxycytidine; dNTP, 2'-deoxynucleoside 5'-triphosphate.

0006-2960/90/0429-2841$02.50/0